Analytical and numerical solutions of the Local Inertial Equations

Ricardo Martins[a,b,*], Jorge Leandro[a,b,c], Slobodan Djordjević[d]

[a]MARE - Marine and Environmental Sciences Centre, Department of Civil Engineering, FCT, University of Coimbra, 3004-517 Coimbra, Portugal
[b]IMAR - Institute of Marine Research, FCT, University of Coimbra, 3004-517 Coimbra, Portugal
[c]Institute of Hydrology, Water Management and Environmental Techniques, Ruhr-University Bochum, Germany
[d]Centre for Water Systems, University of Exeter, North Park Road, Exeter EX4 4QF, United Kingdom

Abstract

Neglecting the convective terms in the Saint-Venant Equations (SVE) in flood hydrodynamic modelling can be done without a loss in accuracy of the simulation results. In this case the Local Inertial Equations (LInE), are obtained. Herein we present two analytical solutions for the Local Inertial Equations. The first is the classical instantaneous Dam-Break Problem and the second a steady state solution over a bump. These solutions are compared with two numerical schemes, namely the first order Roe scheme and the second order MacCormack scheme. Comparison between analytical and numerical results shows that the numerical schemes and the analytical solution converge to a unique solution. Furthermore, by neglecting the convective terms the original numerical schemes remain stable without the need for adding entropy correction, artificial viscosity or special initial conditions, as in the case of the full SVE.

Keywords: Numerical models, Analytical solutions, Local Inertial Equations, Dam-Break

1. Introduction

1.1. Governing Equations

One-dimensional models are applicable when there is a dominant flow direction or when a more detailed solution is not necessary [1]. The SVE equation, as presented by Barré de Saint Venant [2], are a well-accepted mathematical description of the physical phenomenon of a 1D free-surface flow [3] based upon the following assumptions:

- The pressure distribution is hydrostatic (the streamlines have a small curvature and vertical acceleration can be neglected);
- The channel bottom slope is small ($sin(\theta) \approx \theta \wedge cos(\theta) \approx 1$);
- The flow is one dimensional, assuming uniform velocity across the cross-section;
- Friction and turbulence are introduced by assuming laws applicable to steady state flow;
- Water density is constant.

The equations form a system of coupled non-linear hyperbolic partial differential equations that are described by two dependent variables [3], commonly h (water depth) and v (velocity) but also A (cross section area) or z (water level) and q (unit-discharge), related to two independent variables: x, t (longitudinal direction and time). The system of equations can be further simplified. Using the formulation as described by Vázquez-Cendón [4], assuming a constant width of 1, derived from the conservative form, the equations become:

$$\frac{\partial}{\partial t}h + \frac{\partial}{\partial x}q = 0 \tag{1}$$

$$\frac{\partial}{\partial t}q + \frac{\partial}{\partial x}\left(\frac{q^2}{h}\right) + \frac{g}{2}\frac{\partial}{\partial x}h^2 = gh(S - J) \tag{2}$$

h is the water depth, q the unit-discharge and g the gravitational acceleration, S the bed slope and J the friction slope. Some analytical solutions for simplified cases exist but for practical application numerical methods are preferred [5].

In order to reduce the computational time or increase the stability, the SVE are frequently simplified into other models (e.g. Kinematic Wave Model (KWE), Diffusive wave model and Local Inertial Model (LInE)). The LInE is a simplification of the SVE which assumes that the convective terms are negligible. These terms may cause numerical oscillations near discontinuities and wet-dry fronts [6, 7]. Equations (1) and (2) become:

$$\frac{\partial}{\partial t}h + \frac{\partial}{\partial x}q = 0 \tag{3}$$

$$\frac{\partial}{\partial t}q + \frac{g}{2}\frac{\partial}{\partial x}h^2 = gh(S - J) \tag{4}$$

1.2. SVE Analytical Solutions

Analytical solutions are sought mainly for their ability to attest the convergence and correctness of numerical models when

*Corresponding author
Email addresses: Ricardo.Martins@dec.uc.pt (Ricardo Martins), Jorge.Leandro@ruhr-uni-bochum.de (Jorge Leandro), S.Djordjevic@exeter.ac.uk (Slobodan Djordjević)

a full analytical solution for the problem does not exit. A brief historical review of SVE Dam-Break characteristic based analytical solution is presented herein.

SVE Dam-Break analytical solutions are among the most sought solutions. One of the first solutions was presented by Barré de Saint Venant [2] and Ritter [8] for the Dam-Break problem with a dry front. This solution is a parabola that describes the depth of water after the sudden complete breaking of the dam and is based upon the assumption of a prismatic channel with horizontal bed and infinite length and no bed friction. The initial conditions are of a predefined depth upstream of the dam site and no water downstream. The breaking of the dam is assumed to be total and instantaneous. This situation leads to a horizontal asymptote making the propagation in the tip very fast. Dressler [9], by transforming the equations into diffusive wave equations, or, Whitham [10], by treating the tip as a "boundary layer", proposed that the tip of the front wave had a different configuration other than the asymptote. Ritter [8] solution was used and only the tip was changed. Stoker [11] presented the solution for the Dam-Break for a non-wet front where a shock wave or bore travelled forward and a rarefaction wave backwards with a constant depth connecting the shock wave and the beginning of the shock wave. Stoker's Solution also incorporated Ritter [8]'s solution if the depth downstream was assumed to be equal to 0. Hunt [12, 13, 14] proposed an approximate solution based on the kinematic wave for an infinite wet prismatic channel with slope [12], for a sloped prismatic channel with variable width [14] and for an infinite sloped prismatic channel by using the method of asymptotic expansions. Hunt's work mainly focused on the long waves and is only valid after the wave travelled some distance downstream. More recently Mangeney et al. [15] found a solution for the 1D sloped Dam-Break with friction using the Method of characteristics and applied it to avalanches. Ancey et al. [16] presented a solution for steep slopes.

The aim of this work is to: a) present two analytical solution, for the Dam-break problem based on LInE equations by using the Method of characteristics and a steady state solution b) compare the analytical solutions with two numerical solutions of first and second order, with and without shock capturing ability. In the Methodology, the formulae for the depth and velocity will be derived and explained along with the wave propagation characteristics for the Dam-Break. Well established numerical schemes will be applied to the LInE, and compared to the analytical solutions. In the last section conclusions will be drawn about the propagation, analytical solutions and numerical schemes.

2. Methodology

2.1. Analytical Dam-Break Solution

The DamBreak problem can be seen as a Riemann problem which is a fundamental tool to find the characteristics of a set of hyperbolic equations [17]. The initial conditions are constant with a single jump discontinuity at some point [17] usually x =0$[m]$ and described by:

$$h(x,0) = \begin{cases} h_l & if \quad x < 0 \\ h_r & if \quad x > 0 \end{cases} \tag{5}$$

The solution of the Dam-break for the hyperbolic non-linear LInE Equations (Equations (3) and (4)) is obtained through the Method of Characteristics (MOC) that is derived from the geometric theory of the quasi-linear differential equations. MOC provides an insight into the physical behaviour and the construction of an analytical solution [18]. In order to derive the analytical solution of the Dam-Break for the LInE two major steps are defined: (1) calculation of the characteristics and the Riemann Invariants; (2) calculation of the depth and velocity for entire domain.

2.1.1. Step 1 - LInE Characteristics and Riemann Invariants

The concept of Riemann invariants and characteristics is of the utmost importance to understand the propagation of the waves in a set of hyperbolic equation. Equations (6) and (7) show the conservative form of the homogeneous LInE without source terms and in an horizontal, rectangular constant breadth unitary channel (i.e. by neglecting the bed friction and elevation source terms).

$$\frac{\partial}{\partial t}h + \frac{\partial}{\partial x}uh = 0 \tag{6}$$

$$\frac{\partial}{\partial t}uh + \frac{g}{2}\frac{\partial}{\partial x}h^2 = 0 \tag{7}$$

To obtain the Riemann Invariants and the characteristics it is first necessary to linearise the previous set of equations and transform them into a celerity- velocity formulation [18]. From equations (6) and (7) by applying the chain rule we obtain:

$$\frac{\partial}{\partial t}h + h\frac{\partial}{\partial x}u + u\frac{\partial}{\partial x}h = 0 \tag{8}$$

$$h\frac{\partial}{\partial t}u + u\frac{\partial}{\partial t}h + gh\frac{\partial}{\partial x}h = 0 \tag{9}$$

With the celerity $c = \sqrt{gh}$, differentiating c in time and space one obtains:

$$\frac{\partial}{\partial t}c = \frac{\partial}{\partial t}\sqrt{gh} = \frac{g}{2\sqrt{gh}}\frac{\partial}{\partial t}h = \frac{g}{2c}\frac{\partial}{\partial t}h \implies \frac{\partial}{\partial t}h = \frac{2c}{g}\frac{\partial}{\partial t}c \tag{10}$$

$$\frac{\partial}{\partial x}c = \frac{\partial}{\partial x}\sqrt{gh} = \frac{g}{2\sqrt{gh}}\frac{\partial}{\partial x}h = \frac{g}{2c}\frac{\partial}{\partial x}h \implies \frac{\partial}{\partial x}h = \frac{2c}{g}\frac{\partial}{\partial x}c \tag{11}$$

Multiplying (8) by cg and (9) by g and introducing (10) and (11) into (8) and (9), adding and subtracting the equations one obtains:

$$\frac{\partial}{\partial t}(2c^3 + 3uc^2) + c\frac{\partial}{\partial x}(2c^3 + 3uc^2) = 0 \tag{12}$$

$$\frac{\partial}{\partial t}(2c^3 - 3uc^2) - c\frac{\partial}{\partial x}(2c^3 - 3uc^2) = 0 \tag{13}$$

These equations have the form:

$$\frac{\partial}{\partial t}R + \frac{dx}{dt}\frac{\partial}{\partial x}R = 0 \tag{14}$$

With $R = 2c^3 + 3uc^2$ or $R = 2c^3 - 3uc^2$, since $\frac{\partial}{\partial t}R = 0$ along the curves represented by the equation $\frac{dx}{dt} = c$ or $\frac{dx}{dt} = -c$ one obtains:

$$\frac{\partial}{\partial t}(2c^3 + 3uc^2) = 0 \tag{15}$$

On the positive characteristic curves (C^+) with equation:

$$\frac{dx}{dt} = c \tag{16}$$

And:

$$\frac{\partial}{\partial t}(2c^3 - 3uc^2) = 0 \tag{17}$$

On the negative characteristic curves (C^-) with equation:

$$\frac{dx}{dt} = -c \tag{18}$$

On the curves C^+ and C^- the values $2c^3+3uc^2$ and $2c^3-3uc^2$ are the respective Riemann invariants.

2.1.2. Step 2 - Dam-break

In order to derive the analytical solution for the LInE Dam-break - following Stoker [11] - one has to divide the structure of the generic fully developed Dam-Break ($t = t_0$) into 4 areas (Figure 1).

- Area 0 is the downstream condition $depth = h_0$ and $velocity = u_0 = 0$, limited upstream by the steep front wave, which travels with a constant speed ξ.
- Area 1 is upstream condition and has the initial conditions $depth = h_1$ and $velocity = u_1 = 0$. These areas are also the initial condition to the Riemann Problem.
- Area 2 is a zone of constant state with velocity and depth unknown that connects the steep front wave (P_{20}) with the rarefaction waves (P_{13} to P_{32}).
- Area 3 is where the rarefaction waves propagate connecting the constant state 2 with 1.

Areas 1 and 0 are Initial conditions of the problem therefore they are provided, leaving parameters in Areas 2 and 3 to be calculated:h_2 ,u_2 ,ξ h_3 ,and u_3 (c_3 and c_2 are dependent on h_3 and h_2) along with the position of the transition points P_{13}, P_{32}, P_{20}. The points position are obtained in an analogy with the SVE characteristic formulation. The first point is P_{13}, defined by the maximum backwards propagation allowed by the upstream negative characteristic times the time elapsed, we obtain therefore:

$$P_{13} = -c_1 t \tag{19}$$

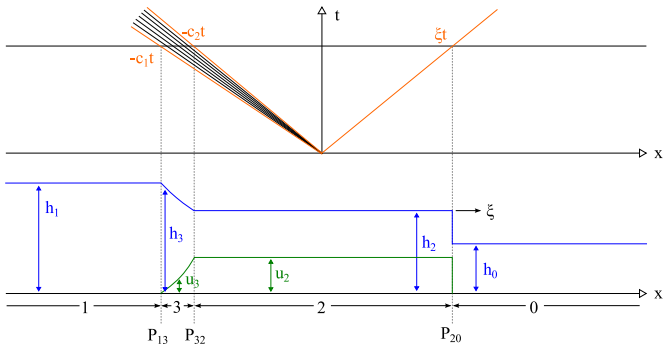

Figure 1: Dam-Break Structure

Since in Area 2 the depth is constant it can be assumed that the last rarefaction wave propagating has the celerity of Area 2 we obtain therefore:

$$P_{32} = -c_2 t \tag{20}$$

For the front steep wave, it has a specific velocity given by ξ present in the relation:

$$P_{20} = \xi t \tag{21}$$

The calculation of depths (or celerities) and velocity will be divided in two sections: (1) parameters in Area 2 and the transition from Area 0 to Area 2; (2) the characterization in Area 3.

The transition from Area 0 to Area 2 is obtained using the two shock conditions for the LInE equations considering the fluid incompressible:

$$h_2(u_2 - \xi) = h_0(u_0 - \xi) \tag{22}$$

$$\xi h_0 u_0 - \xi h_2 u_2 = \frac{1}{2}gh_0^2 - \frac{1}{2}gh_2^2 \tag{23}$$

Equation (22) is obtained from the conservation of mass (6) using the relative velocity U. The relative velocity is the velocity u reduced by the steep front wave propagating velocity ξ ($U = u - \xi$). Equation (23) is obtained from (7) in the same manner. Converting depths to celerities using $h = c^2/g$ and realizing that $u_0 = 0$ one obtains:

$$\frac{c_2^2 u_2}{g} + \xi\frac{c_0^2 - c_2^2}{g} = 0 \tag{24}$$

$$\xi\frac{c_2^2 u_2}{g} - \frac{c_0^4 - c_2^4}{2g} = 0 \tag{25}$$

The system of equations (24) and (25) does not suffice for obtaining the 3 unknowns required: c_2, u_2 ,and ξ. To obtain another equation one must assume that along the positive characteristic curve (C^+) the Riemann Invariant (I^+) remains constant in both Areas 2 and 1 and the velocity in Area 0 is $u_1 = 0$, therefore the following relation is defined:

$$I_2^+ = I_1^+ \implies 2c_2^3 + 3u_2c_2^2 = 2c_1^3 + 3u_1c_1^2 \implies 2c_2^3 + 3u_2c_2^2 = 2c_1^3 \tag{26}$$

Solving for u_2 one obtains:

$$u_2 = \frac{2}{3}\left(\frac{c_1^3}{c_2^3} - c_2\right) \tag{27}$$

Solving the system of Equations (24), (25) ,and (27) one obtains the three variables needed to characterize Area 2 and steep front wave propagation: c_2, u_2 and ξ . This system can be solved using a non-linear iterative method or can be further simplified and provide insight on the wave propagation if we solve equations (24) and (25) for u_2:

$$u_2 = \xi - \xi\frac{c_0^2}{c_2^2} \tag{28}$$

$$u_2 = \frac{c_2^4 - c_0^4}{2\xi c_2^2} \tag{29}$$

Equalling (28) and (29), solving for ξ and neglecting the negative root one obtains:

$$\xi = \sqrt{\frac{c_0^2 - c_2^2}{2}} \tag{30}$$

This shows that the speed of the bore propagation is an average of the squared celerities near the discontinuity. Equation (30) also shows that in case of a wet dry front the steep front wave propagation speed is a function only of the upstream depth. In equation (28) introducing equations (27) that substitutes u_2 and equation (30) that substitutes ξ one gets, after some manipulation:

$$c_2^3 = c_1^3 + \frac{3}{2}(c_0^2 - c_2^2)\sqrt{\frac{c_0^2 - c_2^2}{2}} \tag{31}$$

Solving Equation (31) by iterations and neglecting the irrational roots one obtains c_2 that can be substituted directly in equation (30) and equation (27) to obtain a unique solution. The next step is finding the solution for Area 3 variables. The characteristics (16) and (18) are the solution for the ordinary differential equations (12) and (13) as long as relations (15) and (17) are satisfied. In Area 3 along the negative characteristic (18) we have:

$$c_3 = -\frac{x}{t} \tag{32}$$

Changing variable to h

$$h_3 = \frac{c_3^2}{g} = \frac{x^2}{gt^2} \tag{33}$$

Assuming that the Riemann Invariant (I^+) is kept constant along the positive characteristic curve (C^+) by solving (26) for c_3 and c_1.

$$I_3^+ = I_1^+ \implies 2c_3^3 + 3u_3c_3^2 = 2c_1^3 \implies$$
$$\implies u_3 = \frac{2(c_1^3 - c_3^3)}{3c_2^3} \implies u_3 = \frac{2(c_1^3t^3 + x^3)}{3x^2t} \tag{34}$$

With all the formulae needed to characterize the depth and velocities for the Dam-break, the expressions are given in Tables 1 and 2.

Table 2: Discontinuity point locations in time

	P_{13}	P_{32}	P_{32}
P	$-c_1t$	$-c_2t$	ξt

2.2. Numerical Schemes

For comparison with the Analytical solution two numerical schemes applied to LInE Equations will be presented: (1) a first order in space and time Roe Riemann solver and (2) a second order in time and space McCormack two-step scheme.

Roe. Upwind schemes like the Roe scheme discretize the spatial derivatives so that information is taken from the side it comes rendering these techniques well adapted to advection dominated problems [1]. The set of equations (6) and (6) can be represented in conservative Matrix form as a system of conservation laws as:

$$\frac{\partial}{\partial t}\mathbf{U} + \frac{\partial}{\partial t}\mathbf{F}(\mathbf{U}, x) = 0 \qquad on \qquad \Omega \times [0, t] \in \mathbb{R} \times \mathbb{R}^+ \tag{35}$$

Where Ω is the space domain in $\mathbb{R}$, $[0, t]$ represents the time interval of the solution, $\mathbf{U}$ are the primitives or conserved variables and $\mathbf{F}(\mathbf{U}, x)$ the fluxes given in matrix form by:

$$\mathbf{U} = \begin{bmatrix} h \\ q \end{bmatrix}, \qquad \mathbf{F} = \begin{bmatrix} q \\ \frac{1}{2}gh^2 \end{bmatrix} \tag{36}$$

$q = uh$ is the unit discharge in the x direction (u is the velocity in the x direction), h is the water depth and g is the gravitational acceleration. Roes approximate solver replaces the nonlinear problem in equation (35) by the linearisation:

$$\frac{\partial}{\partial t}\mathbf{U} + \mathbf{A}\frac{\partial}{\partial t}\mathbf{F}(\mathbf{U}, x) = 0, \qquad where \qquad \mathbf{A} = \frac{\partial}{\partial \mathbf{U}}\mathbf{F}(\mathbf{U}, x) \tag{37}$$

This linearization assumes a constant Jacobian $\mathbf{A}$ calculated using consistent and conservative conditions [19].

The discretization is generically represented in Figure 2. Point P is the generic point inside the Domain, O is the point previous to P and Q is the point after P. Discretizing using Roe Scheme [20] and a first order Euler integration for the time one obtains:

$$\mathbf{U}_P^{t+1} = \mathbf{U}_P^t - \frac{\Delta t}{\Delta x}\left[\varphi_{OP} - \varphi_{PQ}\right] \tag{38}$$

Table 1: Formulae used for the Analytical solution of the LInE 1D Dam-break

Area	h	u	c	ξ
1	h_1	0	$c_1 = \sqrt{gh_1}$	–
3	$h_3 = \frac{x^2}{gt^2}$	$u_3 = \frac{2(c_1^3 t^3 + x^3)}{3x^2 t}$	$c_3 = -\frac{x}{t}$	–
2	$h_2 = \frac{c_2^2}{g}$	$u_2 = \frac{2}{3}\left(\frac{c_1^3}{c_2^3} - c_2\right)$	$c_2^3 = c_1^3 + \frac{3}{2}(c_0^2 - c_2^2)\sqrt{\frac{c_0^2 - c_2^2}{2}}$	$\xi = \sqrt{\frac{c_0^2 - c_2^2}{2}}$
0	h_0	0	$c_0 = \sqrt{gh_0}$	–

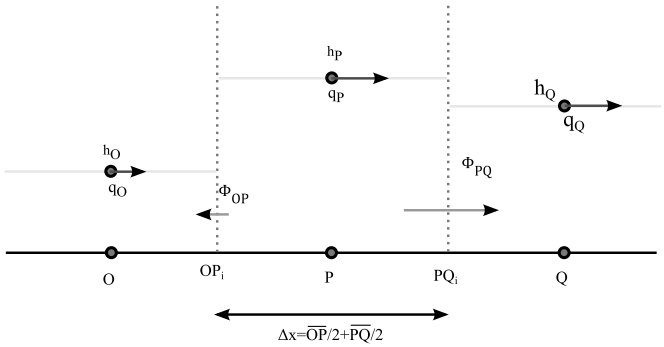

Figure 2: Generic representation of the discretization

With

$$\varphi_{OP} = \left(\frac{\mathbf{F}_O + \mathbf{F}_P}{2} - \left(\frac{1}{2}\mathbf{R}|\mathbf{\Lambda}|\mathbf{R}^{-1}\right)_{OP}(\mathbf{U}_P - \mathbf{U}_O)\right),$$
$$\varphi_{PQ} = \left(\frac{\mathbf{F}_P + \mathbf{F}_Q}{2} - \left(\frac{1}{2}\mathbf{R}|\mathbf{\Lambda}|\mathbf{R}^{-1}\right)_{PQ}(\mathbf{U}_Q - \mathbf{U}_P)\right) \quad (39)$$

With $\mathbf{U}$ and $\mathbf{F}$ obtained for each generic point from equation (36), $\mathbf{R}$ the eigenvectors of $\mathbf{A} = \partial\mathbf{F}(\mathbf{U}, x)/\partial\mathbf{U}$, the Jacobian Matrix of $\mathbf{F}$ and $\mathbf{\Lambda}$ the diagonalized matrix of the right eigenvalues of $\mathbf{A}$. They are therefore for LInE:

$$\mathbf{A} = \begin{bmatrix} 0 & 1 \\ \tilde{c}^2 & 0 \end{bmatrix}, \quad \mathbf{R} = \begin{bmatrix} 1 & 1 \\ \tilde{c} & -\tilde{c} \end{bmatrix},$$
$$\mathbf{R^{-1}} = \frac{1}{2\tilde{c}}\begin{bmatrix} \tilde{c} & 1 \\ \tilde{c} & -1 \end{bmatrix}, \quad \mathbf{\Lambda} = \begin{bmatrix} \tilde{c} & 0 \\ 0 & -\tilde{c} \end{bmatrix} \quad (40)$$

$\tilde{c}$ is the Averaged value of the celerity measured at the interface between two points, that since equal spacing is considered here is assumed as:

$$\tilde{c} = \sqrt{\frac{g}{2}(h_{P_1} + h_{P_2})} \quad (41)$$

Where P_1 and P_2 are generic Points. Since $\tilde{c}$ is always equal or greater than 0, $\mathbf{\Lambda}$ can be explicitly split into two matrices used in equation (38) and equation(39) that consider the incoming and on-going wave strengths and is expressed as:

$$\mathbf{\Lambda}^+ = \begin{bmatrix} \tilde{c} & 0 \\ 0 & 0 \end{bmatrix}, \qquad \mathbf{\Lambda}^- = \begin{bmatrix} 0 & 0 \\ 0 & -\tilde{c} \end{bmatrix} \quad (42)$$

After some manipulation, by introducing the values between points (using (41) with P_1 and P_2 as O,P,Q) and introducing the Matrices (40) and (42), Equation (38) and (39), by equalling the source terms to the fluxes in hydrostatics conditions (the well balancing C-property (Conservation Property)) the updated depth and discharge finally becomes:

$$h_P^{t+1} = h_P^t + \frac{\Delta t}{2\Delta x}$$
$$\left(\delta q_{OP} + \delta h_{OP}^t \tilde{c}_{OP} + \delta h_{QP}^t \tilde{c}_{PQ} - \delta z_{PQ}\tilde{c}_{PQ} + \delta z_{OP}\tilde{c}_{OP}\right) \quad (43)$$

and

$$q_P^{t+1} = q_P^t + \frac{\Delta t}{2\Delta x}$$
$$\left(\frac{g}{2}\delta h_{O^2P^2}^t + \delta q_{OP}^t \tilde{c}_{OP} + \delta q_{QP}^t \tilde{c}_{PQ} - \delta z_{PQ}\tilde{c}_{PQ}^2 + \delta z_{OP}\tilde{c}_{OP}^2\right) \quad (44)$$

with

$$\delta q_{OP}^t = q_O^t - q_P^t, \quad \delta h_{OP}^t = h_O^t - h_P^t, \quad \delta h_{QP}^t = h_Q^t - h_P^t,$$
$$\delta z_{PQ} = z_P - z_Q, \delta z_{OP} = z_O - z_P, \quad \delta h_{O^2P^2}^t = {h_O^t}^2 - {h_P^t}^2,$$
$$\delta q_{QP}^t = q_Q^t - q_P^t \quad (45)$$

Roe scheme, for the SVE, may allow non-physical numerical solutions [17]. This is due to an entropy violation where shock waves are created where rarefaction waves should exist. The entropy violation is attributed to the fact that a linearised Riemann solver (like Roe approximate Riemann solver) solution does not consist of continuous rarefaction waves but discontinuities [17]. These discontinuities causes instabilities when the rarefaction eigenvalue is close to zero ($u - c$ for a positive velocity and $u + c$ for a negative velocity), namely when the velocity is close to the celerity and the negative eigenvalue of the SVE becomes close to zero (e.g. stationary hydraulic jump). The SVE eigenvalues or wave speeds ($u + c$ and $u - c$)

accept three possible states of flow: Supercritical, Subcritical and Critical (See 3 (SVE)) that depend on the velocity u, the direction of flow and the celerity $c = \sqrt{gh}$ being h the depth. LInE only accepts one state as seen in Figure 3 (LInE) dependent upon $c = \sqrt{gh}$. Since the wave speeds for LInE are always far from zero, the rarefaction wave is well pronounced and has no entropy violation.

MacCormack. McCormack Scheme is a well-established second order in time and space two-steps Numerical Scheme. The form used in this paper is the one presented by MacCormack [21] adapted to LInE and has as a predictor step:

$$\begin{bmatrix} h_P^{t+1/2} \\ q_P^{t+1/2} \end{bmatrix} = \begin{bmatrix} h_P^t - \dfrac{\Delta t}{\Delta x}\delta q_{QP}^t \\ q_P^t - \dfrac{\Delta t}{\Delta x}\dfrac{g}{2}\delta h_{Q^2P^2}^t - \dfrac{\Delta t}{\Delta x} g h_P^t \delta z_{QP} \end{bmatrix} \tag{46}$$

Followed by a corrector step:

$$\begin{bmatrix} h_P^{t+1} \\ q_P^{t+1} \end{bmatrix} = \begin{bmatrix} \dfrac{1}{2}\left(h_P^t + h_P^{t+1/2} - \dfrac{\Delta t}{\Delta x}\delta q_{PO}^{t+1/2}\right) \\ \dfrac{1}{2}\left(q_P^t + q_P^{t+1/2} - \dfrac{\Delta t}{\Delta x}\left(\dfrac{g}{2}\delta h_{P^2O^2}^{t+1/2} + g h_P^{t+1/2}\delta z_{PO}\right)\right) \end{bmatrix} \tag{47}$$

with

$$\begin{aligned} &\delta z_{QP} = z_Q - z_P, \quad \delta h_{Q^2P^2}^t = {h_Q^t}^2 - {h_P^t}^2, \quad \delta q_{QP}^t = q_Q^t - q_P^t, \\ &\delta q_{PO}^{t+1/2} = q_P^{t+1/2} - q_O^{t+1/2}, \quad \delta h_{P^2O^2}^{t+1/2} = {h_P^{t+1/2}}^2 - {h_O^{t+1/2}}^2, \\ &\delta z_{PO} = z_P - z_O \end{aligned} \tag{48}$$

MacCormack scheme, for the SVE, usually requires the use of artificial viscosity, limiters, or a smoothing of the initial conditions to converge to the correct solution [22]. The LInE, on the contrary, requires no additional change or corrections.

2.3. Evaluation

In order to numerically evaluate the results L2-norm (Equation (49)) [23] and Pearson product-moment correlation coefficient (Equation (50)) [24] were used.

$$L2 = \sqrt{\frac{\sum_{i=1}^{n}\left(x_i^{Num} - x_i^{Ana}\right)^2}{\sum_{i=1}^{n} x_i^{Ana\,2}}} \tag{49}$$

$$R = \frac{\sum_{i=1}^{n}\left(x_i^{Ana} - \overline{x_i^{Ana}}\right)\left(x_i^{Num} - \overline{x_i^{Num}}\right)}{\sqrt{\sum_{i=1}^{n}\left(x_i^{Ana} - \overline{x_i^{Ana}}\right)^2\left(x_i^{Num} - \overline{x_i^{Num}}\right)^2}} \tag{50}$$

Where n is the total size of the sample, i a random point of the sample, x_i^{Num} and x_i^{Ana} a numerical or analytical value respectively for point i and $\overline{x_i^{Num}}$ and $\overline{x_i^{Ana}}$ are the averages respectively of the numerical and analytical values.

3. Results and Discussion

3.1. Steady State Verification

Another analytical solution is obtained through the conservation of energy throughout the domain. The test comprises a domain with 25 metres, with a relatively small bump near the middle where a steady state is established. The flow, has a Froude number smaller than 1 and is therefore a test in subcritical regime. The boundaries in the test have critical importance. A flow of $q = 4.42[m^3/s]$ is defined at the upstream boundary whilst the depth of $h_D = 1.58514[m]$ is given at the downstream end. The time step is related to the CFL condition and the distance step is $0.1[m]$. The bed elevation is defined by:

$$\zeta(x) = \begin{cases} 0 & if \quad x \leq 8[m] \\ 0.2 - 0.05(x-10)^2 & if \quad 8 < x < 12[m] \\ 0 & if \quad x \geq 12[m] \end{cases} \tag{51}$$

Bottom friction is considered null. Since the test is performed until steady state flow, the Bernoulli equation applied to the LInE (the convective terms neglected) is applicable as:

$$\frac{\partial}{\partial x}H = 0 \underbrace{\Longrightarrow}_{\text{SVE}} \frac{\partial}{\partial x}\left(z + h + \frac{u^2}{2g}\right) = 0 \underbrace{\Longrightarrow}_{\text{LInE}} \frac{\partial}{\partial x}(z+h) = 0 \tag{52}$$

LInE Energy, is known for the downstream boundary condition, therefore, since the bed elevation z in the right boundary is 0, $H = h_D$. Using (52) one obtains the depth for all points and using continuity $q = uh$ we can obtain the velocity. The comparison of the results for the head and velocity are presented in Figure 4.

A dry bed is used as the initial condition. Roe scheme achieved steady state convergence for a difference in domain volume of $10^{-10}[m^3]$ whilst MacCormack never achieved the convergence. This situation is due to the explicit source term treatment and second order nature that induces numerical spurious oscillations. The errors are negligible as seen in Table 3 L2-norm coefficient where for the Roe scheme the error is close to the machine precision whilst for MacCormack the values are close to 10^{-3}.

Table 3: L2-norm for Roe and MacCormack Schemes compared to the Steady state analytical solution

	$L2_{Roe}$	$L2_{Mac}$
Hydraulic Head	1.353×10^{-09}	1.061×10^{-04}
Velocity	9.231×10^{-10}	2.893×10^{-03}

3.2. Application to the Dam-break problem

In order to verify the analytical solution a Dam-Break test was performed with different initial conditions. The test is composed of a 2000 meters long channel divided in half by a gate at x=0 $[m]$. Bed elevation is 0 $[m]$ and the friction was neglected.

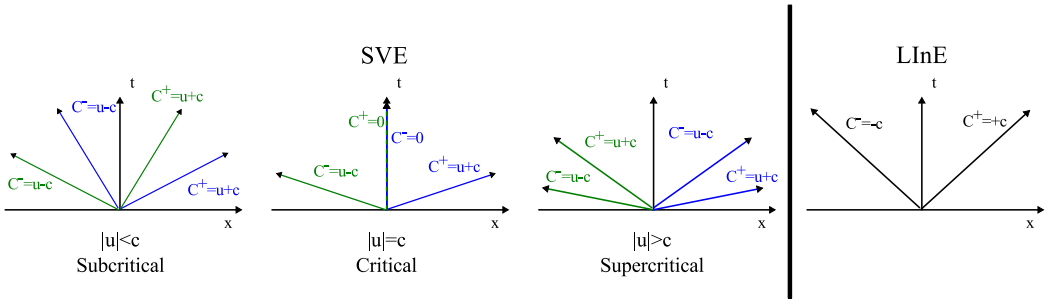

Figure 3: Eigenvalues for SVE and LInE

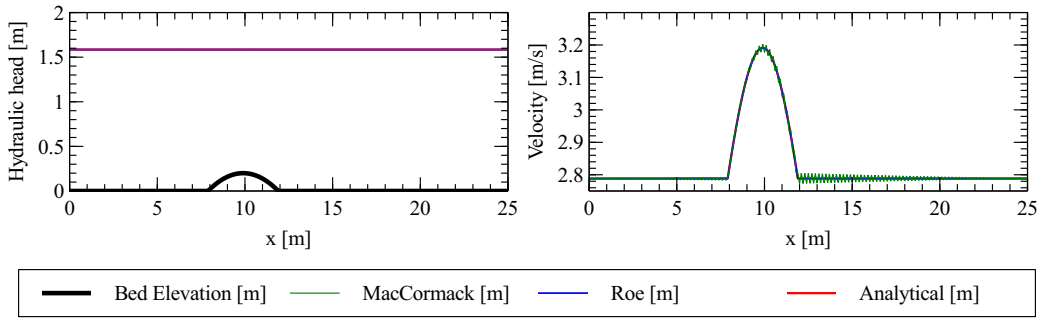

Figure 4: Depth and velocities for the steady state test

The initial velocity is 0 $[m/s]$ on both sides of the gate. The test is conducted by opening the Gate at x =0 $[m]$ (Figure 5).

The expected behaviour is a steep front wave travelling downstream whereas a fan of rarefaction waves should propagate upstream. The test was performed with 10 $[m]$ depth as the upstream initial condition and downstream initial condition varying each metre from 0 to 9 $[m]$ and for t =50$[s]$. Figure 5 shows the Depth and Velocities for the changing downstream initial depth.

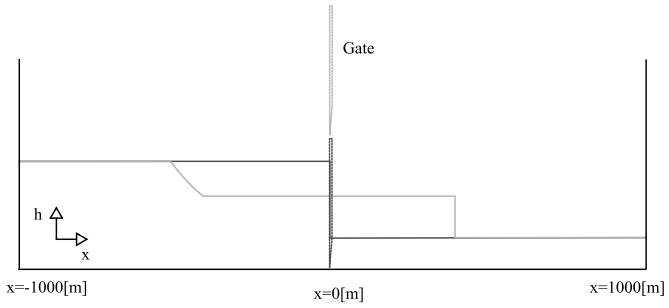

Figure 5: Dam-Break configuration Initial condition: dark grey

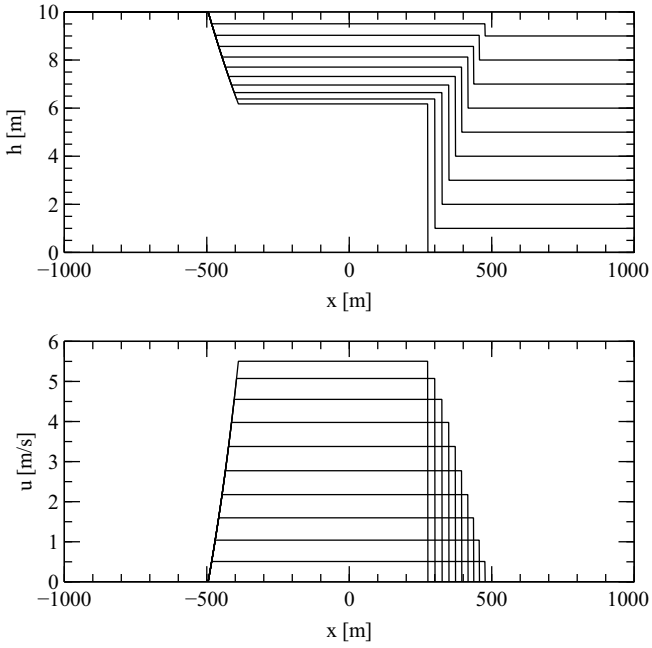

Figure 6: Depth and velocities for a varying downstream condition: h from 0 to 9 $[m]$. t =50 $[s]$

In Figure 6 it should be noticed that although the velocity is greater for the lower depth in the downstream condition, the steep front wave propagation is slower, this is because the front wave propagation is not a function of the velocity but a function of the depth upstream and downstream of the Shock Wave (see Equation (30)).

Two downstream conditions were studied in more detail for comparison with numerical schemes: (1) a wet downstream (WD) condition and (2) a dry downstream (DD) condition. Upstream the depth is 10 metres and downstream it is 5 $[m]$ in the WD test and 0 metres in the DD test. The tests were conducted for Roe and MacCormack schemes. Depths and velocities for DD are presented in Figure 7, and for WD in Figure 8.

In Figure 7 one can see the depth (left) and velocity (right) for the two numerical schemes used and the analytical solution.

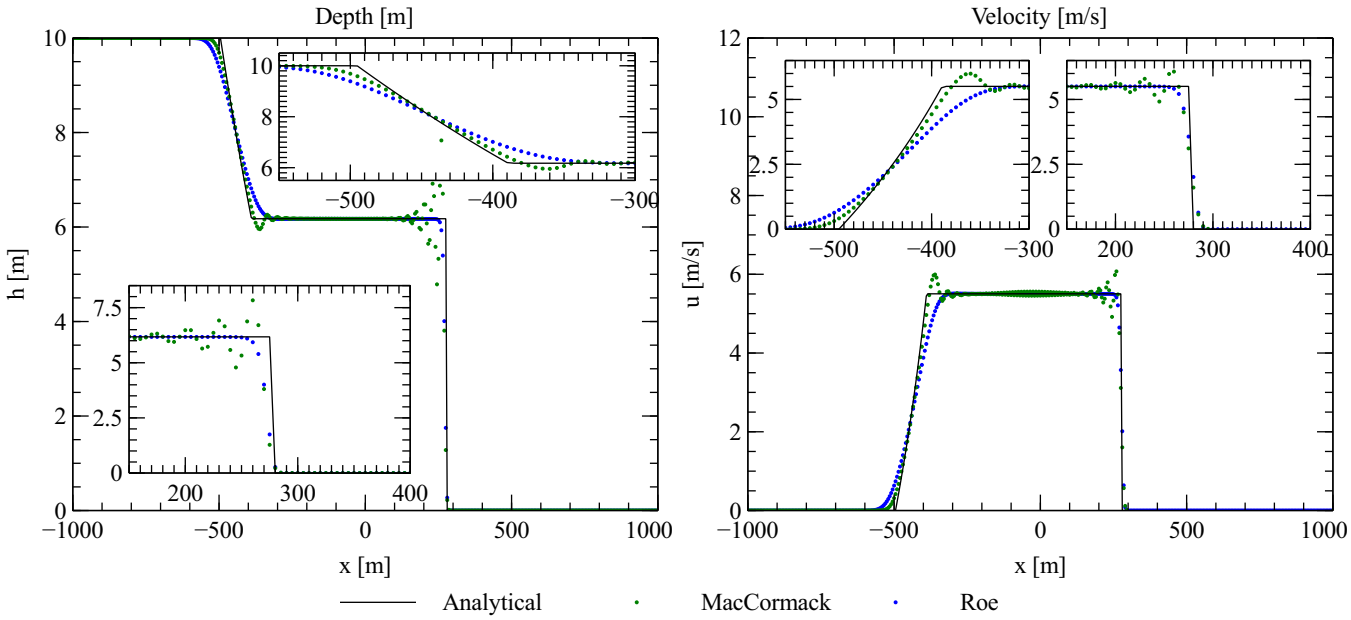

Figure 7: Depth and velocities profiles for t=50[s] with hd=0[m]

The Figures also present details on the Rarefaction waves location and the Shock wave for the depth (Shock Lower left corner, Rarefaction Upper right corner) and velocity (Shock Upper right corner, Rarefaction Upper left corner). Results are similar between the numerical and the analytical solution and the location of the steep front wave and the rarefaction is approximate. The reason being the relatively coarse mesh used of 5 $[m]$.

Figure 8 shows the depth and velocity for the WD condition. The disposition in Figure 8 is the same as in Figure 7. The comparison clearly demonstrates the similarity between the analytical and the numerical results. In the first order Roe scheme some damping is observed whereas in MacCormack there are some oscillations near discontinuities. Except for the spurious oscillations, MacCormack scheme is closer to the analytical solution than the Roe scheme as expected since the former is a second order scheme. It should also be noticed that when comparing the steep front wave with the MacCormack scheme the results in Figure 7 show more oscillations than the ones in Figure 8 showing that the steeper the wave front (higher gradient) the higher are the spurious oscillations in the 2nd order scheme. The results for L2-norm and Pearson coefficient are presented in Table 4.

Table 4: L2-norm and Pearson Correlation

$h_{downstream}$	R_{Roe}	R_{Mac}	$L2_{Roe}$	$L2_{Mac}$
5	0.9966	0.9978	0.0203	0.0163
0	0.9977	0.9971	0.0427	0.0483

The results show a very good agreement between the values obtained by the numerical and the analytical model. The lower correlation value obtained in the Pearson product-moment correlation coefficient is 0.9904. The higher value is 0.9978. The L2-norm errors results are similar to the correlation coefficient in terms of convergence. The higher value is 0.072 whereas the lower value is approximately 0.016.

4. Concluding Remarks

In this paper an analytical solution based on the method of characteristics and a steady state analytical solution were presented for the Local Inertial Model (LInE) set of equations, along with a first order in space and time Roe Scheme derived for the LInE and MacCormack scheme applied to the LInE. Unlike with SVE the MacCormack and Roe schemes applied to the LInE did not need the commonly applied entropy correction, artificial viscosity or special initial conditions to remain stable. However, MacCormack scheme showed some oscillations in steady state with source terms. The results showed a very good agreement between the analytical and the numerical solutions. The analytical solutions can thus be used to validate numerical models based on the LInE.

5. Acknowledgements

The first author thanks and acknowledges the contribution of FCT (Portuguese Foundation for Science and Technology) through the Doctoral Grant SFRH/BD/81869/2011 financed through the POPH/FSE (Programa Operacional Potencial Humano/Fundo Social Europeu) program.

References

[1] P. García-Navarro, P. Brufau, J. Burguete, J. Murillo, The shallow water equations: An example of hyperbolic system, Monografias de la Real Academia de Ciencias de Zaragoza 31 (2008) 89–119.

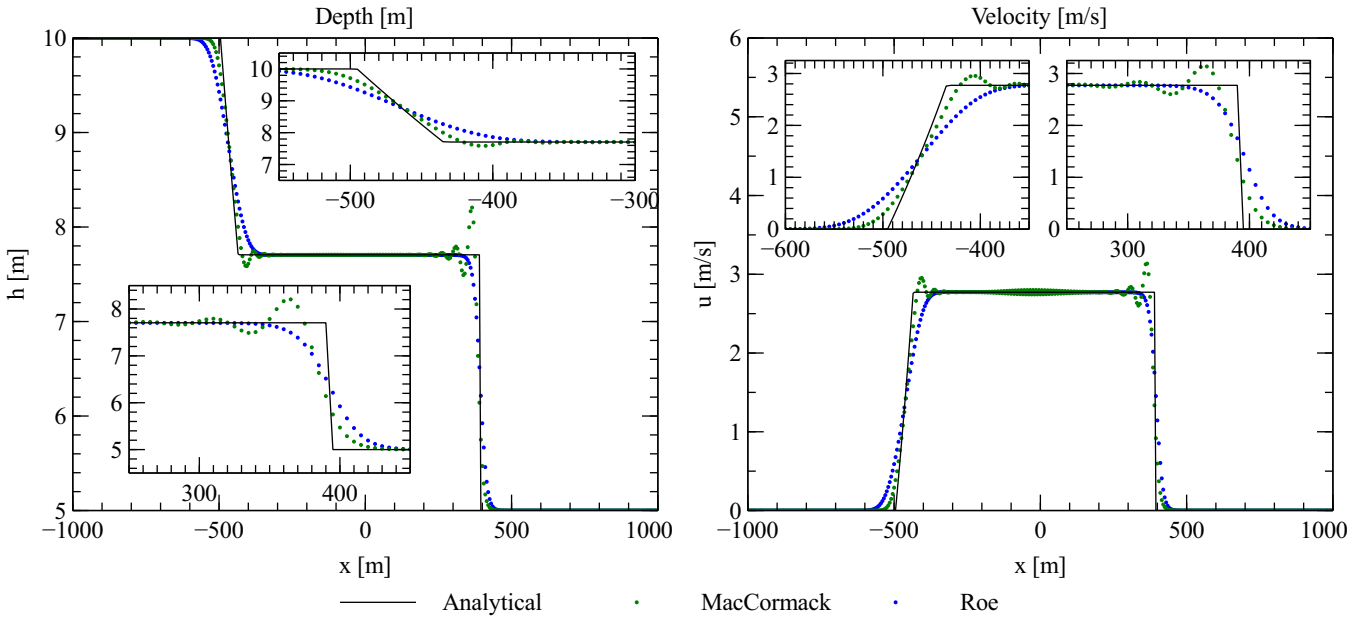

Figure 8: Depth and velocities profiles for t=50[s] with hd=5[m]

[2] A. Barré de Saint Venant, Théorie et Equations Générales du Mouvement Non Permanent des Eaux Courantes., Comptes Rendus des Séances de l'Académie des Sciences 73 (1871) 147–154.

[3] J. Cunge, F. Holly, A. Verwey, Practical aspects of computational river hydraulics, Pitman Publishing Limited, London, 1980.

[4] M. Vázquez-Cendón, Improved Treatment of Source Terms in Upwind Schemes for the Shallow Water Equations in Channels with Irregular Geometry, Journal of Computational Physics 148 (1999) 497–526. doi:10.1006/jcph.1998.6127.

[5] M. H. Chaudhry, Open-channel flow, 2th ed., Springer Verlag, 2008.

[6] G. Aronica, T. Tucciarelli, C. Nasello, 2D multilevel model for flood wave propagation in flood-affected areas, Journal of Water Resources Planning and Management 124 (1998) 210–217.

[7] R. Martins, J. Leandro, S. Djordjević, A well balanced Roe Scheme for the local inertial equations with an unstructured mesh, Advances in Water Resources 83 (2015) 351–363. doi:10.1016/j.advwatres.2015.07.007.

[8] A. Ritter, "Die Fortpflanzung der Wasserwellen." (in German), Vereine Deutscher Ingenieure Zeitswchrift 36 (1892) 947–954.

[9] R. Dressler, Hydraulic Resistance Effect Upon the Dam-Break Functions, Journal of Research of the National Bureau of Standards 49 (1952) 217–225.

[10] G. Whitham, The Effects of Hydraulic Resistance in the Dam-Break Problem., Proceedings of the Royal Society A: Mathematical, Physical and Engineering Sciences 227 (1955) 399–407.

[11] J. J. Stoker, Water waves: the mathematical theory with applications, volume 36, Wiley-Interscience, 1957.

[12] B. Hunt, Asymptotic solution for dam break on sloping channel, Journal of Hydraulic Engineering 109 (1983) 1698–1706. doi:10.1061/(ASCE)0733-9429(1983)109:12(1698).

[13] B. Hunt, Dam-Break Solution, Journal of Hydraulic Engineering 110 (1984) 675–686. doi:10.1061/(ASCE)0733-9429(1984)110:6(675).

[14] B. Hunt, Perturbation Solution for Dam-Break Floods, Journal of Hydraulic Engineering 110 (1984) 1058–1071. doi:10.1061/(ASCE)0733-9429(1984)110:8(1058).

[15] A. Mangeney, P. Heinrich, R. Roche, Analytical solution for testing debris avalanche numerical models, Pure and Applied Geophysics 157 (2000) 1081–1096.

[16] C. Ancey, R. M. Iverson, M. Rentschler, R. P. Denlinger, An exact solution for ideal dam-break floods on steep slopes, Water Resources Research 44 (2008) n/a–n/a. doi:10.1029/2007WR006353.

[17] R. J. LeVeque, Finite volume methods for hyperbolic problems, volume 31, Cambridge Univ Pr, 2002.

[18] J. Hervouet, Hydrodynamics of Free Surface Flows: Modelling with the finite element method, Wiley, 2007.

[19] I. Nikolos, A. Delis, An unstructured node-centered finite volume scheme for shallow water flows with wet/dry fronts over complex topography, Computer Methods in Applied Mechanics and Engineering 198 (2009) 3723–3750. doi:10.1016/j.cma.2009.08.006.

[20] P. Roe, Approximate Riemann solvers, parameter vectors, and difference schemes, Journal of Computational Physics 372 (1981) 357–372. doi:10.1016/0021-9991(81)90128-5.

[21] R. MacCormack, The effect of viscosity in hypervelocity impact cratering, American Institute of Aeronautics and Astronautics (1969) Paper 69–354.

[22] J. Leandro, H. Ramos, Enabling the MacCormack original scheme to perform dam- break flow by fitting a smoothed initial condition on a fixed non-uniform grid, in: 10th International Conference On Pressure Surges, 1, Edinburgh, 2008, p. 15.

[23] G. Lin, J. Lai, W. Guo, High-resolution TVD schemes in finite volume method for hydraulic shock wave modeling, Journal of Hydraulic Research 43 (2005) 376–389.

[24] J. Rodgers, W. Nicewander, Thirteen ways to look at the correlation coefficient, The American Statistician 42 (1988) 59–66. doi:10.1080/00031305.1988.10475524.